Dynamic instrumented palpation (DIP) - a new method for soft tissue quality assessment: Part 1, application to engineered mechanical phantom materials

T.H.J.Yang[1], S.Phipps[2], S.K.W.Leung[2], R.L.Reuben[1†], F.K.Habib[2], S.A.McNeill[3], R.W.Else[4]

[1] Heriot-Watt University, Institute of Mechanical Process and Energy Engineering, School of Engineering and Physical Sciences, Edinburgh, UK.
[2] University of Edinburgh, Prostate Research Group, Edinburgh, UK.
[3] Western General Hospital, Department of Urology, Edinburgh, UK.
[4] University of Edinburgh, Royal School of Veterinary Studies, Edinburgh, UK.

[†] Corresponding Author
Heriot-Watt University
Institute of Mechanical Process and Energy Engineering
School of Engineering and Physical Sciences
Riccarton, Edinburgh, EH14 4AS, UK.
Email: R.L.Reuben@hw.ac.uk

Keywords:
Dynamic instrumented palpation, soft tissue biomechanics, dynamic elastic modulus, silicone, gelatin

Abstract

This paper presents a novel way of assessing the quality of biological tissue for diagnostic purposes, Dynamic Instrumented Palpation (DIP). The method involves applying a controlled modulated strain or displacement to the tissue and measuring the resulting force as a function of time. The method is distinct from dynamic elastography in that the force and displacement are applied and measured by direct mechanical means at relatively low frequency (up to a few tens of Hz) and is more akin to a conventional mechanical test. The dynamic relationship between the force / stress and the strain / displacement is expressed as a function of frequency, this function being the measure to be correlated with tissue quality.

The method is applied here to indentation of a set of engineered phantoms, intended to represent a controlled range of tissue quality, by altering the type and distribution of a harder and a softer phase. In the present work, the phantom tissues were engineered from natural and synthetic sponges impregnated with either silicone or gelatin, although the ultimate application is to human prostate, which can be considered as a biphasic structure (at least at the macro-scale), to distinguish between benign prostate disease and cancer.

The work demonstrates that a range of frequencies can be used to yield a characteristic for the material which depends not only on the material type(s) but also on the morphology of the constituents. The method, therefore, shows good promise for application to the identification of multicomponent soft tissue make-up. As such, it is complementary to dynamic elastography, and its value lies in it being deployable *in vivo* as an adjunct during minimally invasive interventions. Future work will be aimed at establishing the capability of the method on human prostate tissue both *in vitro* and *in vivo*.

1. Background

It is well-known, and somewhat intuitive, that the mechanical properties of biological tissue depend on the microscopic and macroscopic molecular structure and, importantly, the types of cells within the material as well as the way in which they are arranged. Most early work, for example Fung [1], on the elastic properties of soft tissue was focused on components such as such as elastin, collagen, and actin where the interest is largely on behaviour in tension, and, whereas each component has its unique mechanical properties, the relationship between structure and properties is of lesser interest. Interest in the relationship between structure and properties in soft tissue has traditionally centred around elastography [2], where the aim is to provide contrast between (usually) benign, or normal, tissue and that affected by cancer. Because of the delivery method in elastography, much of the development study has used compression and because of the need to assess image contrast, only static or quasi-static measures of elastic modulus were made at the outset, e.g. Krouskop *et al*. [3], often without a clear indication of strain rate and/or strain range, both of which are likely to affect the measurement. There is a growing acceptance that the viscoelastic (or, at least, non-linear elastic) properties of biological materials are of diagnostic significance, e.g. Zhang *et al*. [4]. However, most of the recent published work is focused on applications to elastography with the main aim of maximising

contrast. The current work focuses on low frequency direct mechanical assessment of tissue, essentially as an instrumented version of palpation.

Manual palpation has been used for centuries to detect nodules under the skin or embedded within an organ and a number of devices have been developed to instrument this technique, either in order to provide a permanent record or to reach areas that cannot be easily accessed with the hand or finger. Most systems measure load (or pressure) resulting from an applied displacement, which can be manual, as is the case for those aimed at tissue quality assessment [e.g. 5, 6], or automatic, usually used for robotic surgery-assist devices [e.g. 7, 8]. Mostly, these devices record a static or quasi-static material response (single value of elastic modulus or stiffness) and the few vibratory probes that exist [e.g. 9, 10] invariably search for a resonant frequency and seek to correlate that with a diagnosis.

Figure 1 illustrates the essential principle of dynamic instrumented palpation for a general biphasic biological material in which one component is relatively elastic and the other is relatively viscous (Figure 1a). An oscillatory indentation displacement is applied to the material and the resulting force recorded as a function of time. Once any transients have died away, the force response is also a sinusoid (Figure 1b) so that the phase difference between the load and displacement and the amplitude ratio can be determined to give the complex stiffness: $\tilde{k} = \frac{|F|}{|\delta|} e^{i\omega t+\varphi}$ and the ratio of the amplitudes of force to displacement and the phase lag are the primary indicators of the material response, Figure 1c. The quasi-static stiffness (ratio of mean force to mean displacement) can also be recorded. It is normal to suppose that the force is linearly related to stress and the displacement to strain so the complex stiffness is proportional to complex modulus.

For testing a given material, the mean level, the amplitude and the frequency of the applied displacement can all be varied, although it is advisable to keep the amplitude relatively small to obtain a near-sinusoidal force response in the quasi-stationary state. Generally speaking, altering the mean value of displacement reveals any non-linearity in the stress-strain response, and using a large enough pre-compression can be important for sensitivity [3] as many biological materials exhibit very shallow stress strain curves at low strains. However, the most important experimental variable is frequency and, as can be seen from Figure 1(c), the way in which the phase lag and amplitude ratio vary with frequency as well as the choice of frequency range can be important in discriminating between different proportions and types of components in the tissue. Figure 1(c) was calculated for a hypothetical 3-component standard linear solid viscoelastic constitutive model shown in general multicomponent form in Figure 2. For this simple model, the quasi-stationary phase lag and amplitude ratio are:

$$\tan\varphi = \frac{\frac{\eta}{E_1}\omega}{\frac{E_2}{E_1} + \left(\frac{\eta}{E_1}\right)^2 \left(1+\frac{E_2}{E_1}\right)\omega^2} \qquad \frac{AR}{E_2} = \sqrt{\frac{\left[\frac{E_2}{E_1} + \left(\frac{\eta}{E_1}\right)^2 \left(1+\frac{E_2}{E_1}\right)\omega^2\right]^2 + \left(\frac{\eta}{E_1}\right)^2 \omega^2}{\left(\frac{E_2}{E_1}\right)^2 \left[1+\left(\frac{\eta}{E_1}\right)^2 \omega^2\right]}}$$

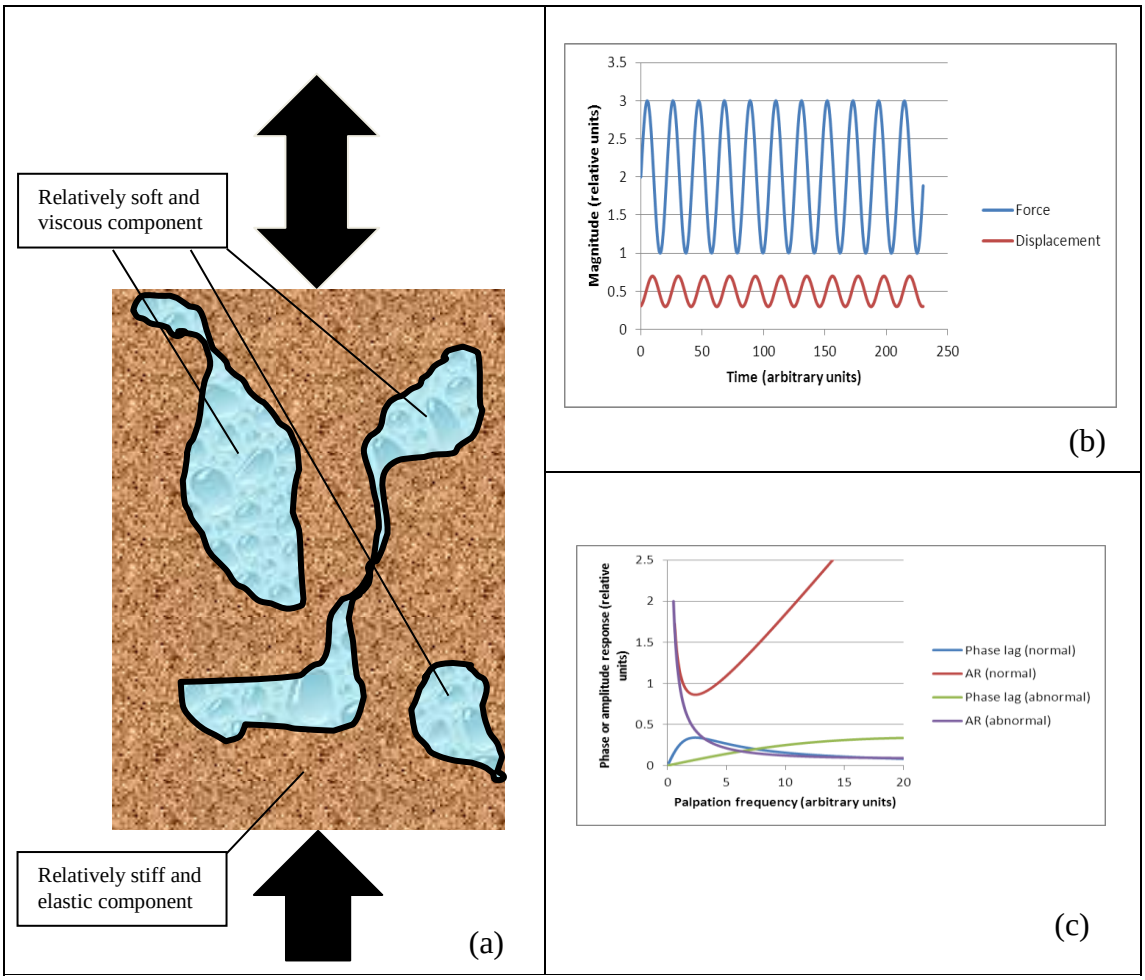

Figure 1: Essential principle of dynamic instrumented palpation (DIP): (a) schematic of loading and structure of solid, (b) relationship between steady-state time-series of displacement and load, (c) hypothetical response curves for phase lag and amplitude ratio in normal and abnormal tissue.

In the tissue labelled as "abnormal" in Figure 2, the viscous modulus, η, has been reduced, as might be expected to occur, say, in the case of inflammation or benign prostatic hyperplasia (BPH). The volume probed by a given indenter may contain one or more viscoelastic elements and these elements may each have different parameters, so the relationship with frequency could, in principle, become quite complicated [11]. Even for the relatively simple (3-parameter, two stiffness, single viscosity) model used to calculate the responses in Figure 1c, the variation of phase lag and/or amplitude ratio with frequency need not be monotonic. Also, the concept (and hence the method) is scalable, and can be applied from the cell level [12] right up to the whole organ level [13]. A basic hypothesis of the method is that the viscous behaviour, and the associated time constants in the stress-strain response, is attributable to the movement of liquid from compressed parts of the structure, in which case one could expect a distribution of time constants which are characteristic of the histological structure at a scale corresponding to the deformed volume associated with the probe.

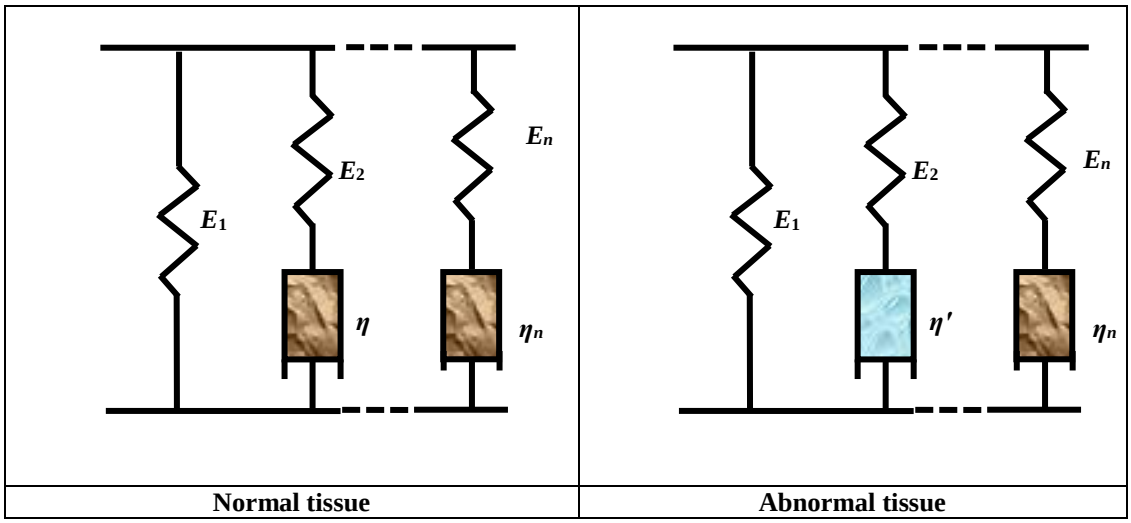

Figure 2: Multicomponent viscoelastic constitutive models.

Of course, the material need not be characterised by any particular viscoelastic model, and the model itself (as opposed to the parameters) may change between individuals, between conditions of the tissue and even from time-to-time in a given individual, for example in response to changes in blood pressure. Also, multiple characteristic times or frequencies may be present [14], and one or more relaxation time may be such that the quasi-stationary state takes many cycles to establish, Figure 3. None of this detracts from the potential of the method to be used for multi-scale characterisation of tissue structure – a "mechanical phenotype" [15], but with the added advantage that the mechanical characterisation is the variation of complex modulus with frequency, a kind of meta-touch. This potential complexty in real tissue means that it is necessary, first of all, to test the method on stuctures which are "engineered", but which have properties, at least superficially, like those of the tissue target.

The ultimate objective of the current work is to instrument *in vivo* clinical palpation, similar to digital rectal examination (DRE) but covering the range of "normal", cancerous and benign hyperplastic conditions. The advantage of DIP here is not just in the instrumentation and improved accessibility, but also in the provision of information than cannot be assessed even by a skilled practitioner. In order to establish a relationship between structure and properties, a measurement system was devised, capable of carrying out cyclic strain-controlled point probing at actuation frequencies between 5Hz and 30Hz on small excised prostate tissue specimens (chips) collected from transurethral resection of the prostate (TURP). The chosen frequency range was arrived at by considering those few studies which have been done (e.g. [3]), the likely time available to make an *in vivo* assessment, and pragmatic observations of recovery times in surface indented human tissue and TURP specimens.

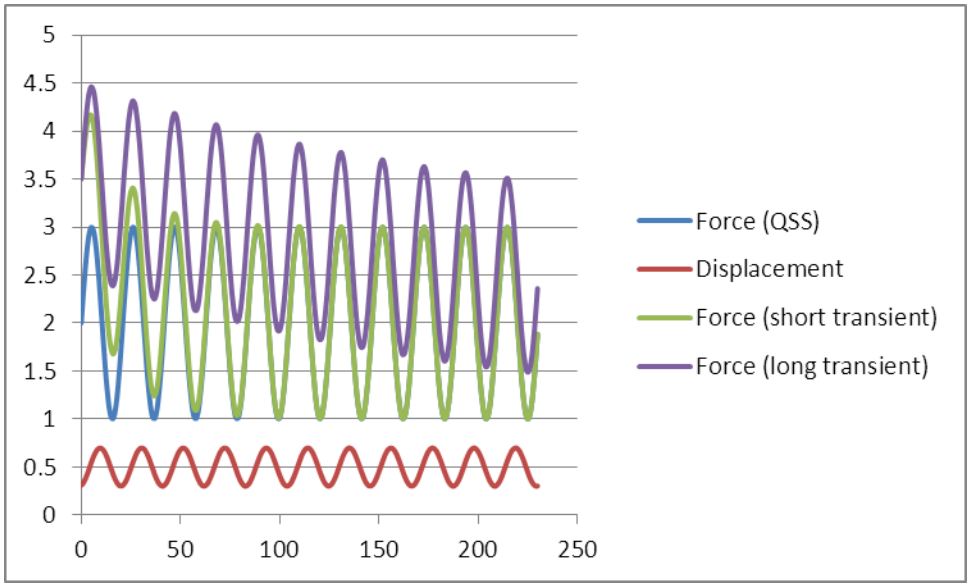

Figure 3: Material response with (additional) long relaxation time(s).

This paper outlines the design of the test system and its calibration using a set of engineered phantoms where the properties of the components and the biphasic make-up could be controlled.

2. Materials and Methods

An impregnation method was used to engineer a material to simulate "two-phase" biological materials in which one component formed the matrix and the other was relatively soft. Synthetic and natural sponge were used as matrix materials and, as can be seen in the scanning electron micrographs in Figure 4, these are open-cell structures with a pore size in the region of 100-600μm, the pores being somewhat larger and more regular in the synthetic sponge. Samples were taken from two of each type of sponge and the gross voidage was estimated by image analysis of micrographs, the two synthetic sponges yielding volume fractions of matrix of 37% and 33% and the natural sponges 16% and 17%, although the variability between microscope frames was greater for the natural than the synthetic sponges. Also, the natural sponge contained a secondary component of micro-voidage not included in the above estimates. The main difference, however, was in the matrix materials; the synthetic sponge, being a soft polymer, does not stiffen when dried out whereas the (mostly collagenous) natural sponge becomes quite hard when dry.

Each type of matrix was impregnated with RTV silicone and, for the synthetic sponge, with gelatin to give three types of biphasic phantom, while specimens of the unreinforced gelatin and silicone were also prepared. The silicone was Silbione RTV 4408 (Bentley Chemicals), a two-part elastomer that crosslinks at room temperature by a polyaddition reaction. The gelatin was 300 bloom from swine skin and was prepared at a concentration of 33g/l by dissolving the powder in warm water and allowing to cool naturally.

Synthetic and natural sponge samples were cut to a nominal size of 10mm × 10mm × 4mm thick (a little larger than prostate chips) and were immersed in a beaker of either warm gelatin or uncured silicone. As the specimens were small, trapped air could be expelled by compressing the sponge against the base of the beaker using a glass stirrer. The impregnating agent was allowed to cure at room temperature and, when fully cured, the resulting block of gelatin or silicone was cut to retrieve the impregnated sponge specimens.

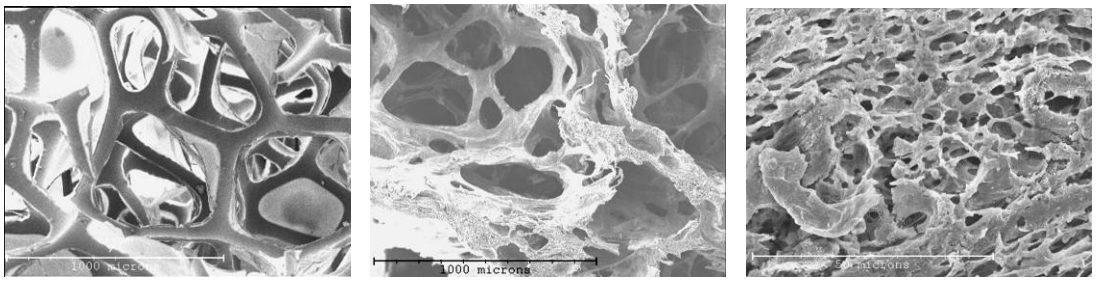

Figure 4: Matrix materials: left - synthetic sponge, middle - natural sponge, right - natural sponge at lower magnification.

The indentation system (Figure 5) consisted of an electromechanical shaker (LDS V201 with amplifier PA-25E) which could be used to induce controlled cyclic displacements of between 0.5mm and 1.0mm amplitude at actuation frequencies between 5Hz and 30Hz. The electromechanical shaker moved a base plate on which the specimen was mounted and the displacement of the baseplate was measured by a proximity probe (Bentley Nevada 3300XL). The cyclic displacement transmitted a force through the specimen and onto a 2.0mm diameter ball-ended probe where a low displacement miniature load cell (Sensotec Model 31) was connected in series.

The output from the load cell was fed into a signal conditioning unit (Measurements Group 2311) and then into a data acquisition system, which also gathered synchronously the output from the proximity probe. The data acquisition system was a multi-function National Instruments 6036E card, which was also used to feed a sinusoidal waveform to the amplifier controlling the electromechanical shaker. Both displacement and force waveforms were collected at a sampling rate of 1.5kS/sec.

Although the proximity sensor and load cell were factory calibrated, a system calibration was carried out by applying a small alternating displacement directly onto the load cell at actuation frequencies between 5Hz and 30Hz, yielding system characteristic calibration factors (Figure 6) for amplitude ratio and phase difference at each actuation frequency which could be applied to the measured readings.

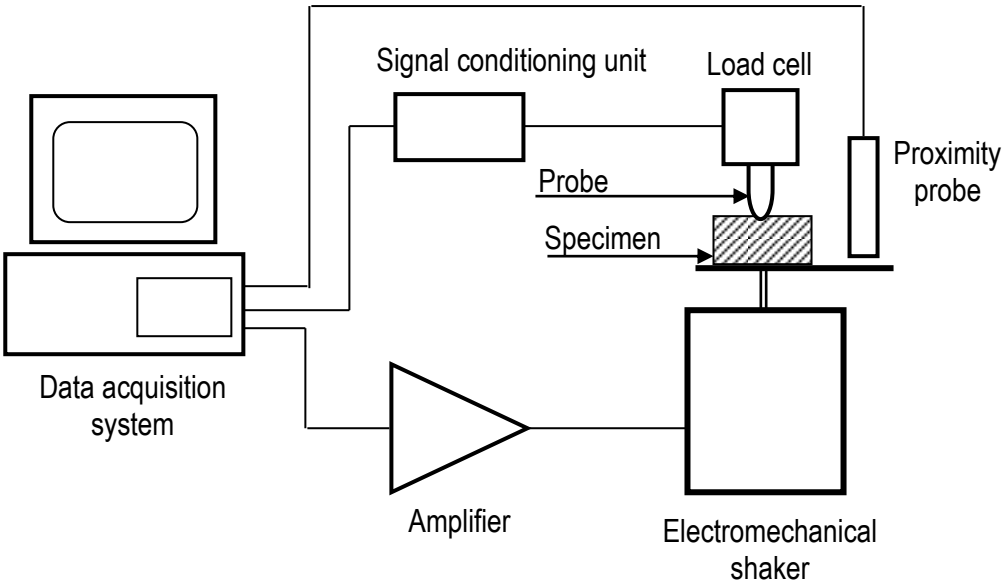

Figure 5: Schematic diagram of dynamic indentation system.

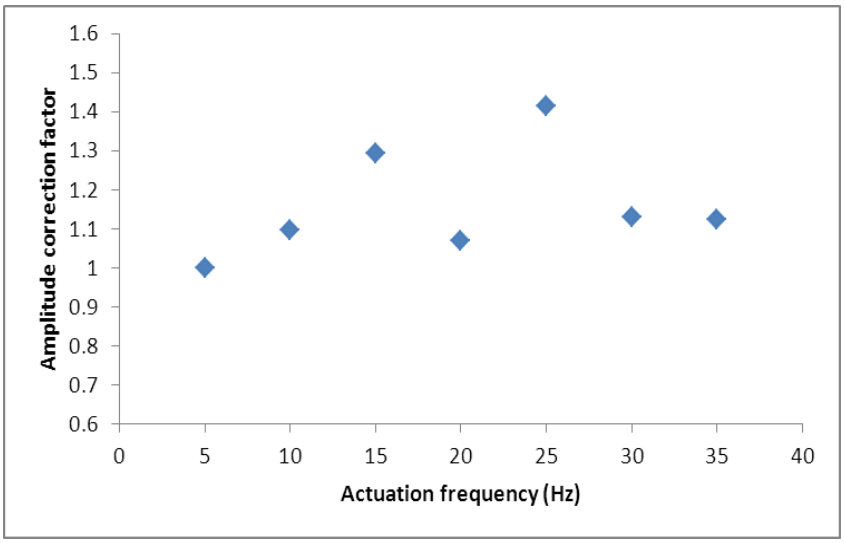

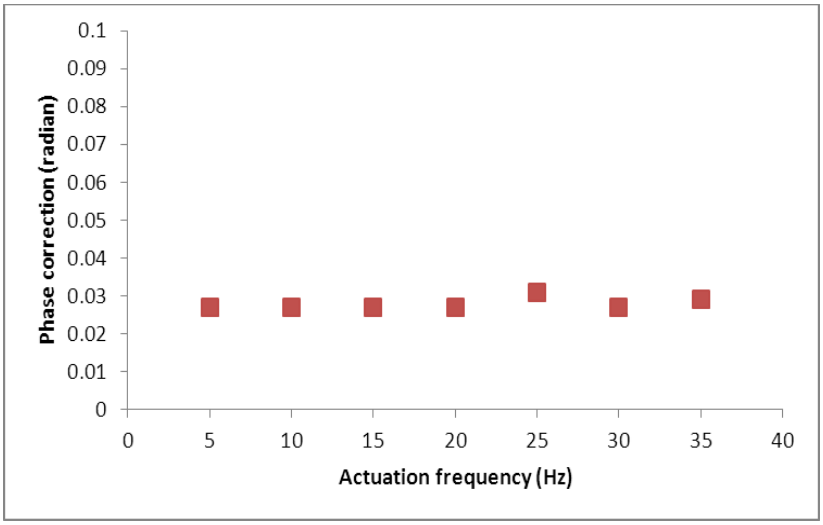

Figure 6: System characteristics of indentation test system

For each sample, typically 50 cycles were acquired at each of the 8 actuation frequencies between 5 and 40Hz. Because the fundamental frequency is known, the amplitudes of displacement and force waveforms could be signal-averaged (taking points one period apart) to obtain a single cycle. Next the first Fourier coefficients and the mean of both displacement and force sinusoidal waveforms were calculated, yielding three measures of each; the amplitude, the phase and the mean. The amplitude and mean were converted to stress $\tilde{\sigma} = \sigma_0 e^{i\omega t}$ and strain $\tilde{\varepsilon} = \varepsilon_0 e^{i\omega t+\varphi}$ simply assuming that the entire sample is compressed uniformly under the projected area of the probe, giving three measures of the modulus.

Mean effective modulus, $E_{eff} = \dfrac{\sigma_{mean}}{\varepsilon_{mean}}$

Amplitude ratio, $\left|E^*(\omega)\right| = \dfrac{\sigma_0}{\varepsilon_0} = \sqrt{E_S^2(\omega) + E_L^2(\omega)}$

Phase difference, $\tan\left[\varphi(\omega)\right] = \dfrac{E_L}{E_S}$

where the storage modulus, E_S and the loss modulus E_L are an alternative way of expressing the complex modulus.

The stress field under the probe is, of course, not uniform [16] and, for samples of large extent relative to the size of the probe and the depth of probing, it is usually to use a Hertzian contact model to assess the modulus [e.g. 3], although this requires the assumption of a value for Poisson's ratio. Ahn and Kim [17, 18] have specifically assessed the implications of the Hertzian contact assumption for large (whole organ) soft tissue samples and have found that the difference from a simulated value is small for softer tissues, becoming larger (although still not highly significant in the face variations due to the diagnostic target) as the tissue stiffness increases. Given that the depth of probing here is between 10 and 25% of the depth of the sample, it was concluded that the added complexity of a full simulation would add little to the essential purpose of the paper, which was to assess how effective modulus varied with palpation frequency and the structure of the phantom.

3. Results

Figure 7 summarises the modulus measurements for the unreinforced silicone and gelatin. Apart from the expected tenfold difference in the magnitude of the modulus, a number of other differences in behaviour of the two materials are seen over the frequency range examined. The amplitude ratio of the silicone shows a monotonic increase of about 50% between 5 and 40 Hz and the mean effective modulus lies close to the low end of the range. By contrast, the amplitude ratio for the gelatin shows a modest decrease (about 12%) over the frequency range and the mean effective modulus is significantly lower than the lowest frequency value of amplitude ratio. The phase differences for the two materials also exhibit distinct evolutions with frequency, that for gelatin increasing sharply between 5 and 20Hz and rather less between 20 and 40Hz. For silicone, the phase difference decreases to a minimum at 25Hz, increasing thereafter.

(a)

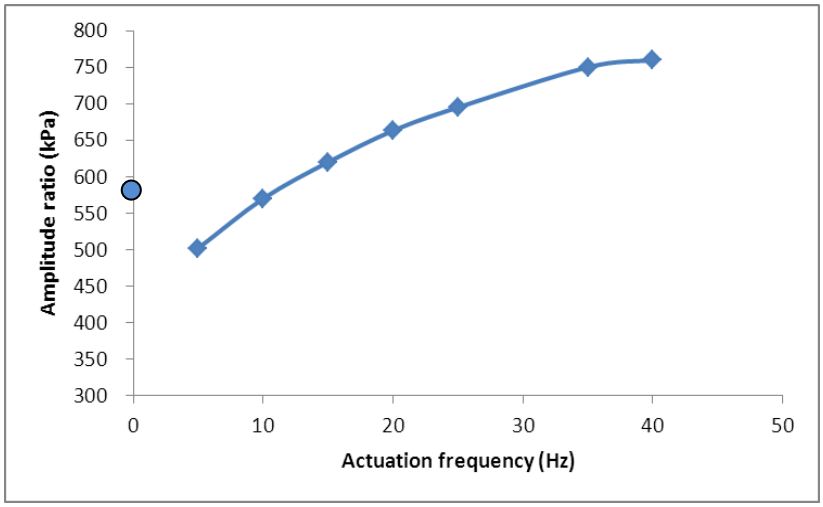
Amplitude ratio (kPa)
800
750
700
650
600
550
500
450
400
350
300
0
10
20
30
40
50
Actuation frequency (Hz)

(b)

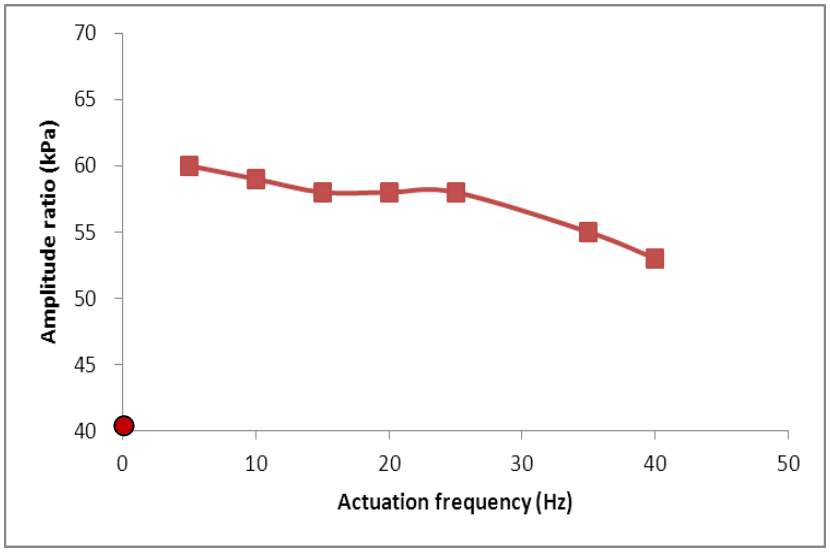
Amplitude ratio (kPa)
70
65
60
55
50
45
40
0
10
20
30
40
50
Actuation frequency (Hz)

(c)

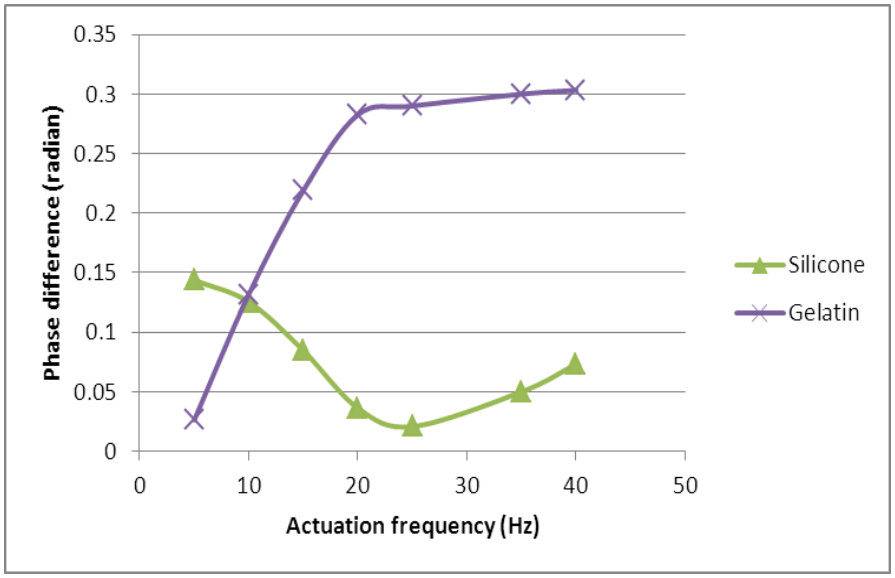

Figure 7: Modulus of unreinforced silicone and gelatin; (a) amplitude ratio and mean effective modulus (single point) for silicone, (b) amplitude ratio and mean effective modulus (single point) for gelatin, (c) phase difference for silicone and gelatin.

The sponges confer some further interesting behaviour on the silicone and gelatin, Figure 8. All of the amplitude ratios for silicone-impregnated sponges follow a similar evolution to unreinforced silicone, but with a distinct maximum within the frequency range of observation. The natural sponge provides more reinforcement than the synthetic sponge despite there being less of it as a percentage of the composite. The gelatin-impregnated sponge amplitude ratio follows a similar evolution to the unreinforced gelatin, with a modest continuous decrease over the frequency range. The phase lags for the silicone-impregnated sponges are of similar shape to the unreinforced silicone, but with a sharper rise than decline and with a minimum whose position varies with the amount and type of sponge. Both samples of gelatin-reinforced sponge show a continual increase from almost zero, but without the saturation that occurred at higher frequencies with the unreinforced gelatin.

(a)

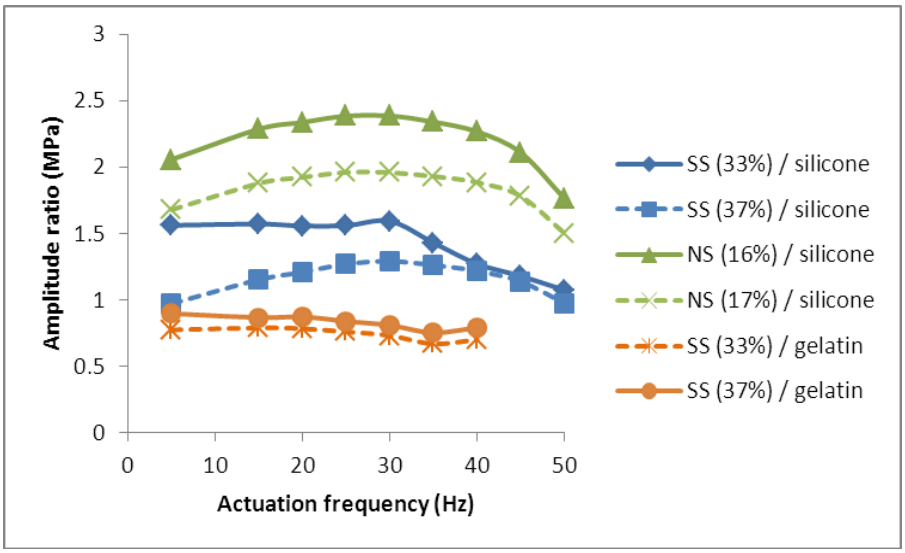

(b)

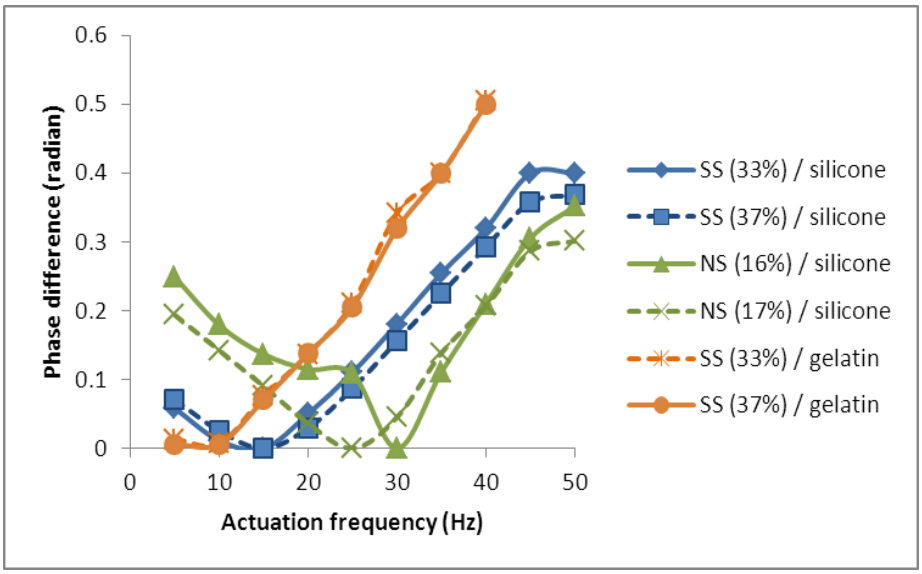

Figure 8: Modulus of sponge-reinforced silicone and gelatin formulations; (a) amplitude ratio, (b) phase difference.

4. Discussion

Gelatin and silicone are widely used as phantom materials for human tissue and a range of test methods using wave propagation and relatively slow indentation have been used to characterise these materials. However, each class of material can be prepared according to a custom formulation and it is difficult to find even static data which is sufficiently general to make a comparison.

Figure 9 shows the measurements from the current work on gelatin, compared with the published data. One of the most extensive studies of the elastic properties of

gelatin (and agar) gels is due to Hall *et al*. [19], who were developing phantoms for elastography. These authors used a similar dynamic compression technique to that used here, with slightly lower strain amplitude and a significantly lower frequency (0.4Hz). They assumed the gel to behave in a linear elastic fashion and, for a gelatin-water ratio of 33g/litre, found the effective Young's modulus (E_{eff}) to be 51.5kPa, which is close to the MEM found here. Hall *et al*. also carried out stress relaxation tests on a number of concentrations and found the relaxation curves to be best fitted using 5 exponential decay constants the first three characteristic times of which were 3, 18 and 80 seconds. It is not possible to devise a 3-parameter model with two relaxation times, so the relaxation information was incorporated into a modified four-parameter model by making both moduli equal to E_{eff}. The amplitude ratio and phase lag can then be expressed as functions of frequency:

$$\frac{AR}{E} = \sqrt{\frac{\left[\left(\frac{\eta_1}{E}\right)^4\omega^4 + \left(\frac{\eta_1}{E}\right)^2\left(1+\frac{\eta_1}{\eta_2}\right)\omega^2\right]^2 + \left[\frac{\eta_1}{E}\frac{\eta_1}{\eta_2}\omega + \left(\frac{\eta_1}{E}\right)^3\left(\frac{2\eta_1}{\eta_2}\right)\omega^3\right]^2}{\left\{\left[\frac{\eta_1}{\eta_2} - \left(\frac{\eta_1}{E}\right)^2\omega^2\right]^2 + \left(\frac{\eta_1}{E}\right)^2\left(1+\frac{2\eta_1}{\eta_2}\right)^2\omega^2\right\}^2}}$$

$$\text{and} \quad \tan\varphi = \frac{\frac{\eta_1}{\eta_2} + \left(\frac{\eta_1}{E}\right)^2\left(\frac{2\eta_1}{\eta_2}\right)\omega^2}{\left(\frac{\eta_1}{E}\right)^3\omega^3 + \left(\frac{\eta_1}{E}\right)\left(1+\frac{\eta_1}{\eta_2}\right)\omega}$$

For this model, the stress relaxation constants are related:

$k_{1,2} = \frac{E}{2\eta_1} + \frac{E}{\eta_2} \mp \sqrt{\frac{E^2}{4\eta_1^2} + \frac{E^2}{\eta_2^2}}$ and, setting $k_{1,2} = \frac{1}{3}, \frac{1}{18}$ allowed the functions to be plotted as shown in Figure 9. Clearly, the amplitude ratio is insensitive to frequency in the range measured here according to this model, and the phase difference is almost zero across all of the range, rising sharply only at low frequencies. Due to the constraints on the model, it was not possible to exhibit any other combinations of the first three relaxation times. Later work by the same group [20] has used a hyper-elastic model for gels in order to take into account the variation in modulus with strain. Qiang *et al*. [21] have measured the response of gelatin phantoms to a Rayleigh wave impulse and report values of the parameters of a Kelvin-Voigt viscoelastic model for 10g/l and 15g/l gelatin gel phantoms. Later, these same authors [22] have compared Kelvin-Voigt parameters measured by impulse and by indentation-relaxation and were able to reproduce the same values of *E*, although they were unable to measure η. Their choice of a Kelvin model is rather odd since it does not exhibit stress relaxation, although it does produce an oscillatory solution to the constitutive equation:

$$\tan\varphi = \frac{\eta}{E}\omega \qquad \frac{AR}{E} = \sqrt{\left(\frac{\eta}{E}\right)^2\omega^2 + 1}$$

which is shown for both sets of reported parameters in Figure 9. As can be seen both the amplitude ratios and phase differences are very low and the values quoted for

Young's modulus by the same authors (37 and 110 kPa) for the two concentrations, illustrate that high frequency measurements based on wave propagation cannot readily be extrapolated to lower palpation frequencies. Madsen *et al*. [23] used a proprietary dynamic test machine to obtain viscoelastic properties of a range of gelatin-agar elastography phantoms. They reported values of storage modulus in the region of 20-60kPa at 1Hz, coupled with rather low phase angles (0.03-0.09 radian) and these are shown in Figure 9 along with some quasi-static measurements [24] made on the same formulation of gelatin as used in the current work at displacement rates of 0.028, 0.036 and 0.22 mm/s, chosen to match the range of maximum displacement rate in the oscillatory tests.

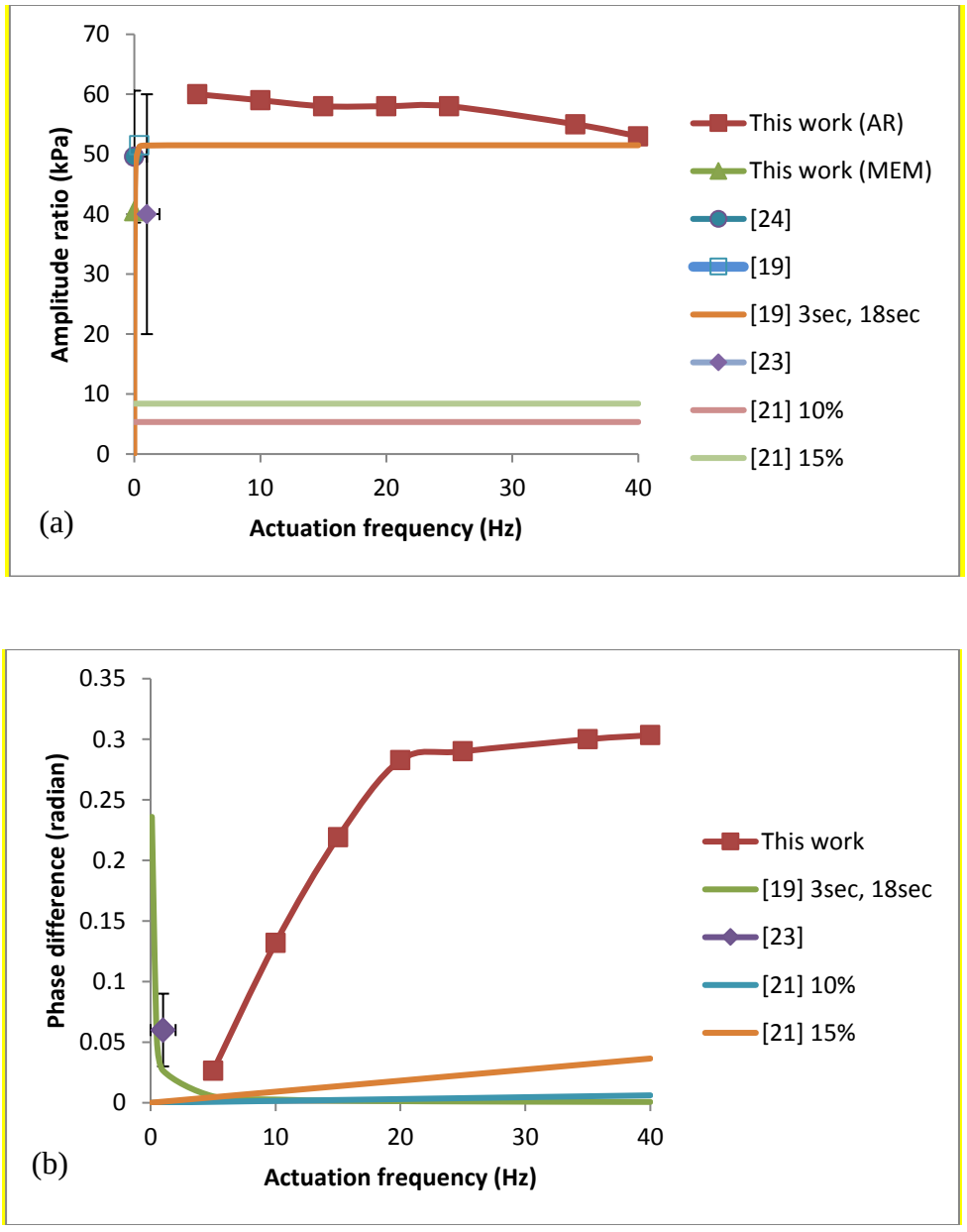

Figure 9: Modulus of gelatin compared with literature; (a) amplitude ratio and mean effective modulus (on vertical axis), (b) phase difference.

Recently, Okamoto *et al*. [25], have carried out dynamic mechanical shear tests in parallel with magnetic resonance elastography measurements on soft gels made from 2.8 % w/w gelatin in a 50/50 mixture of glycerol and water. They fitted their data to three viscoelastic models, including the Kelvin-Voigt and SLS models mentioned above, giving values for the storage and loss shear moduli at 20Hz and 400Hz. The storage modulus was found to be around 1kPa, and to be a relatively weak function of frequency, rising by about 5% per 100Hz, rather less than the difference indicated by the alternative models. The loss modulus was rather lower varying between about 50Pa and 250Pa between 20 and 400Hz, the mechanical shear and MRE measurements diverging increasingly in the range of measurement overlap (between 100Hz and 200Hz). These figures serve to help illustrate that, even with a single formulation of "engineered" material, the method of measurement, the frequency and the choice of any viscoelastic model all affect the result and, for diagnostic purposes, it is probably more helpful to rely on calibration and relative measurements rather than attempt to devise a material model.

Figure 10 shows the measurements from the current work on silicone, compared with other published data. Liang *et al*. [26] have used optical coherence elastography, assuming a Kelvin model, to measure elastic properties of RTV-615 silicones with various ratios of curing agent. Their values for the softest and hardest of these are shown in Figure 10, alongside their measurements using a commercial indentation apparatus (taken to be a static modulus). They did not quote Kelvin parameters, but give the modulus for step- waveforms (essentially impulse response, hence of high frequency) and 20Hz. Peters *et al*. [27], also working with hard and soft silicone breast tissue phantoms, cyclically compressed 74mm diameter cylinders at a frequency of 100Hz. They tracked surface motions and then used a finite element simulation to determine the best fit storage modulus and damping ratio (E_s and ζ), comparing with a measured static storage modulus (slope of linear portion of stress-strain curve between 2% and 10% strain). Figure 10 shows the values of the static modulus as well as the complex modulus $\left|E^*\right| = E_s\sqrt{1+\zeta^2}$ for hard and soft phantoms, the range corresponding to two assumed values of Poisson's ratio, 0.45 and 0.49. Santawisuk *et al*. [28] have measured storage and loss moduli at 1Hz of a range of silicone formulations as candidate denture soft lining materials. The softest of these, Silastic® MDX4-4210, had a modulus in the range of phantom materials and, accordingly, this data is included in Figure 10. Finally, as part of a study on electrorheological materials, Hao *et al*. [29] have reported the storage modulus and loss modulus of 50%/50% RTV silicone/silicone oil 45%/45%/10% RTV silicone/silicone oil /starch mixtures at actuation frequencies of 0.1, 1 and 10Hz. For both materials, they observed an increase in loss modulus at higher frequencies, and a much more modest increase in storage modulus, the effects in both cases being more pronounced for the softer formulation (without starch). These data are shown along with the others in Figure 10. As for the gelatin, and notwithstanding the differences in formulation, it seems that there is reasonable agreement between this work and published data, but only if the measurement conditions (frequency and/or strain rate) are similar. Extrapolations from outside the range in which a measurement was taken are usually unreliable.

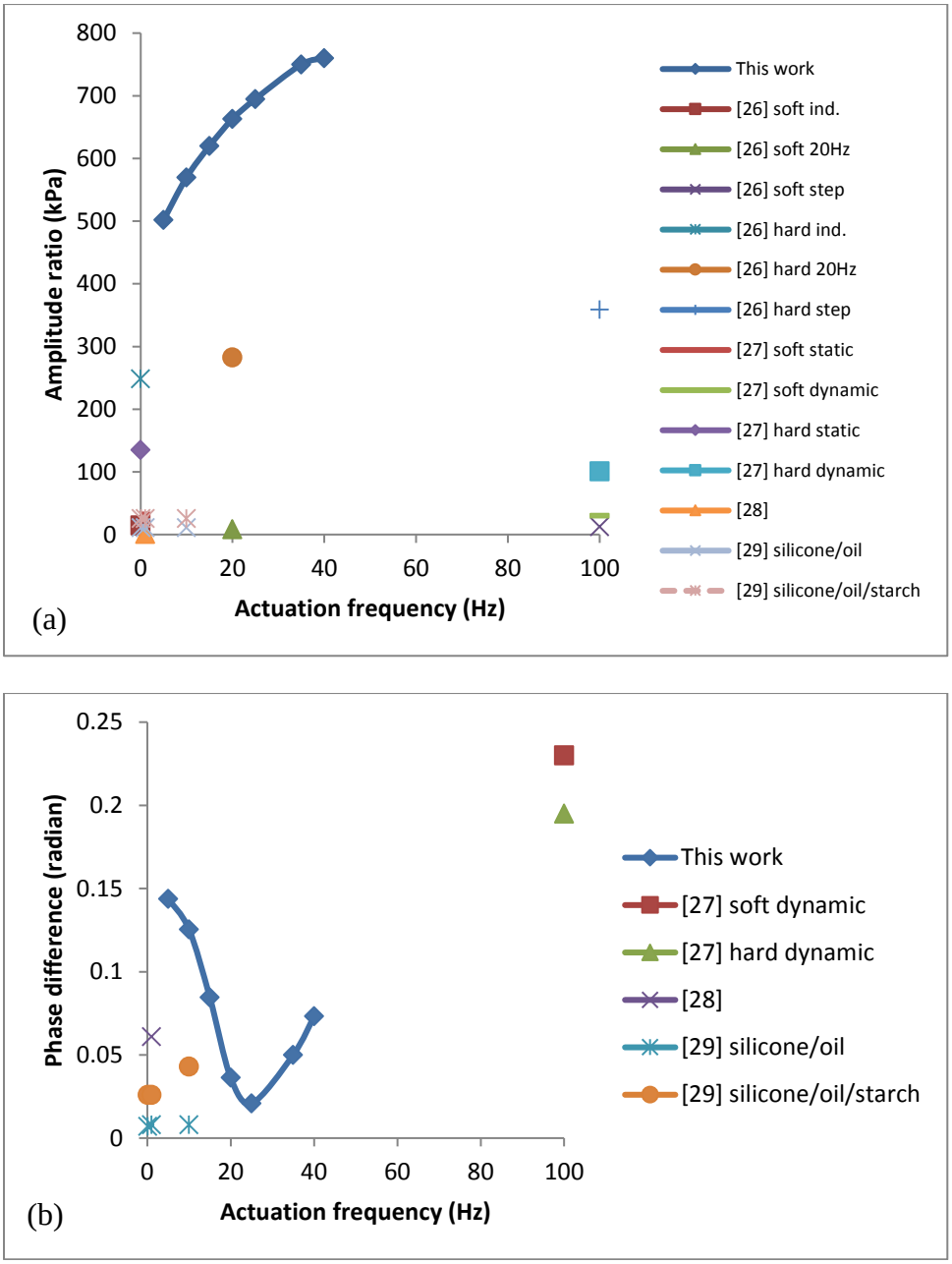

Figure 10: Modulus of silicone compared with literature; (a) amplitude ratio and mean effective modulus (on vertical axis), (b) phase difference.

Figures 11 and 12 show the effect of sponge on the dynamic modulus of gelatin and silicone, respectively. For both gelatin and silicone, the sponge increases the magnitude of the amplitude ratio, and changes the shape of the both the amplitude ratio and phase response with frequency. The effects are different for different sponges and, in the phase in particular, the variation with frequency can be a more important discriminator of structure than the absolute difference at a given frequency. This is illustrated most effectively for the synthetic sponge / silicone combination, where the effect on amplitude ratio is relatively modest, especially at higher

frequencies, and where the minimum in the phase difference is shifted to lower frequencies. These curves illustrate that the more complex nature of the composite is reflected in a different dynamic behaviour only fully revealed when a range of frequencies is used. Although there are no parallel studies to the current one, similar effects have been seen by Hao *et al*. [29] where significant changes were seen in the storage modulus in silicone/starch/oil composites when the structure of a given formulation was conditioned by the application of an electric field during curing. Also, Santawisuk *et al*.[28] found not only the storage and loss modulus, but also at the phase difference at 1Hz of Silastic® MDX4-4210 to be affected systematically by additions of 2-10 parts per hundred of silica filler.

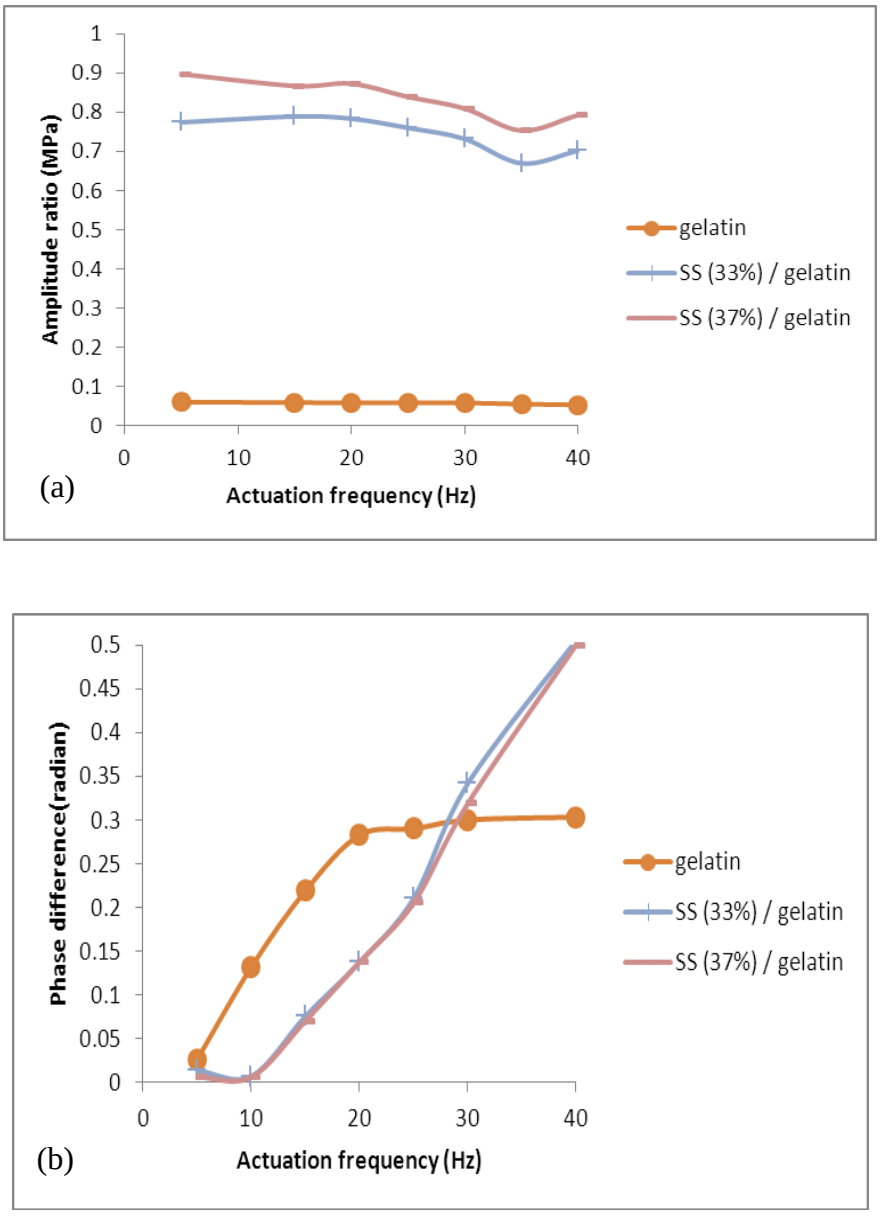

Figure 11: Effect of sponge reinforcement on the modulus of gelatin; (a) amplitude ratio, (b) phase difference.

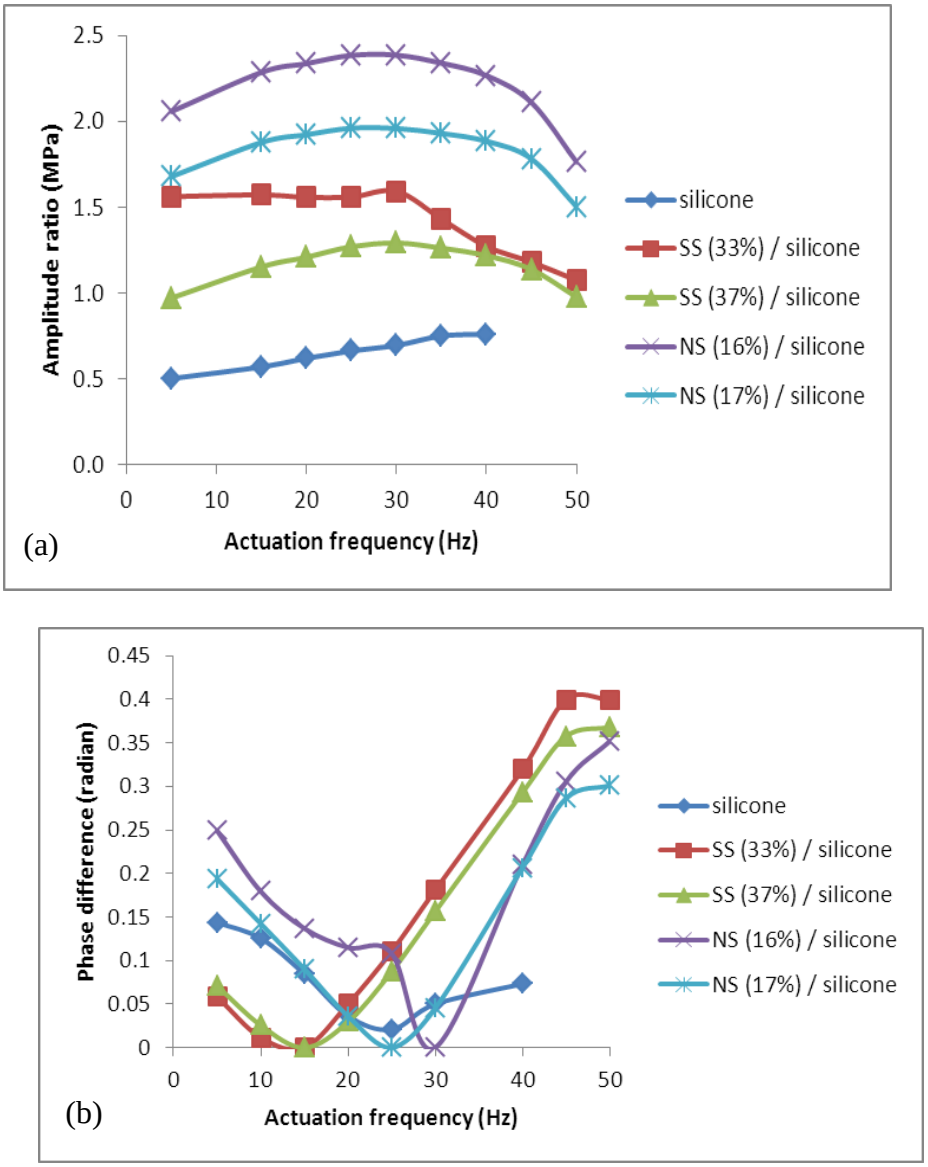

Figure 12: Effect of sponge reinforcement on the modulus of silicone; (a) amplitude ratio, (b) phase difference.

5. Conclusions

This work has demonstrated an approach to measuring the stiffness of soft materials which yields a characteristic behaviour, dependent not only on the material, but also on the structure when the material consists of more than one phase. This behaviour can be investigated by altering the frequency of actuation over a chosen range and is a more efficient means of measuring the dynamic modulus than, say, stress relaxation tests.

Measurements on single phase materials also show characteristic behaviour which is broadly in accord with the limited amount of published data, discrepancies being more likely due to differences in formulation and in different frequencies of actuation.

Generally speaking, extrapolations using viscoelastic models do not lead to any substantial agreement between workers using different strain rates or actuation frequencies, so the quoting of any modulus or viscoelastic parameter is only applicable for the regime in which it was measured.

The introduction of cellular separation of silicone and gelatin using soft and hard sponge matrices indicates that there is some promise that the structure of multi-component biological materials of similar stiffness can be probed using such an approach.

Acknowledgements
This work was supported by the UK Engineering and Physical Sciences Research Council, linked grants GR/R74192, GR/R74215 and GR/R74208: UROCATH – a microengineered tactile urological diagnostic device.

References

1. Fung Y C. "Biomechanics, mechanical properties of living tissues." 2nd ed. 1993, New York: Springer-Verlag. p567.
2. Ophir J, Céspedes I, Ponnekanti H *et al*. "Elastography: a quantitative method for imaging the elasticity of biological tissues", Ultrasonic Imaging, 13, 1991, 111-134
3. Krouskop T A, Wheeler T M, Kallel F *et al*. "Elastic moduli of breast and prostate tissue under compression." Ultrasonic Imaging, 20, 1998, 260-274.
4. Zhang M *et al*. "Quantitative characterization of viscoelastic properties of human prostate correlated with histology", Ultrasound in Medicine and Biology, 34(7), 2008, 1033-1042.
5. Egorov V and Sarvazyan A P. "Mechanical imaging of the breast", IEEE Transactions on Medical Imaging, 27(9), 2008, 1275-1287.
6. Roham H, Najarian S and Hosseini S M. "Design and fabrication of a new tactile probe for measuring the modulus of elasticity of soft tissues", Sensor Review, 27(4), 2007, 317-323.
7. Dario P and Bergamasco M. "An advanced robot system for automated diagnostic tasks through palpation", IEEE Transactions on Biomedical Engineering, 35(2), 1988, 118-126.
8. Bummo A, Park K, Lee H *et al*. "Robotic palpation system for prostate cancer detection", Proceedings 3rd IEEE International Conference on Biomedical Robotics and Biomechatronics, Tokyo, September 2010, 644-649.
9. Baumann I, Plinkert P K, Kunert W *et al*. "Vibrotactile characteristics of different tissues in endoscopic otolaryngologic surgery – *in vivo* and *ex vivo* measurements", Minimally Invasive Therapy and Allied Technologies, 10(6), 2001, 323-327.
10. Omata S and Terunuma Y. "New tactile sensor like the human hand and its applications", Sensors and Actuators A, 35, 1992, 9-15.
11. Renaud F, Dion J-L, Chevallier G et al. "A new identification method of viscoelastic behaviour: application to the generalized Maxwell model", Mechanical Systems and Signal Processing, 25, 2011, 991-1010.
12. Wu H W, Kuhn T and Moy V T. "Mechanical properties of L929 cells measured by atomic force microscopy: effects of anticytoskeletal drugs and membrane crosslinking", Scanning, 20, 1992, 389-397

13. Hien M, Yang T H J, Reuben R L *et al*. "Dynamic measurement of intraocular pressure using a mechanical model of the human eye.", Studies in Health Technology and Informatics, 133, 2008, 112-122
14. Tohill R, Hien M R, McGuinness N *et al*. "Short-term stress relaxation of porcine periodontal ligament - finding an appropriate visco-elastic model", IFMBE Proceedings, Vol. 25, Proceedings World Congress on Medical Physics and Biomedical Engineering, Munich, September 2009, 335-338
15. Lekka M, Pogoda K, Gostek J *et al*. "Cancer cell recognition – mechanical phenotype", Micron, 43, 2012, 1259-1266
16. Palacio-Torralba J, Hammer S, Good D W *et al*. "Quantitative diagnostics of soft tissue through viscoelastic characterization using time-based instrumented palpation", J. Mech. Behav. Biomed. Mater. 41, 2015, 149-160
17. Ahn B and Kim J. "Measurement and characterization of soft tissue behavior with surface deformation and force response under large deformations", Med Image Anal. 14(2), 2010, 138–48
18. Kim Y, Ahn B, Lee JW, et al. "Local property characterisation of prostate glands using inhomogeneous modeling based on tumor volume and location analysis", Med Biol Eng Comput, 51, 2013, 197-205
19. Hall T J, Bilgen M, Insana M F *et al*. "Phantom materials for elastography. IEEE Transactions on Ultrasonics, Ferroelectrics and Frequency Control, 44(6), 1997, 1355-1365
20. Pavan T Z, Carneiro A A O, Madsen E L *et al*. "Exploring the nonlinear elastic behavior of phantoms materials for elastography", Proceedings IEEE International Ultrasonics Symposium, Rome, September 2009, 463-466.
21. Qiang B, Greenleaf J and Zhang X. "Quantifying viscoelasticity of gelatin phantoms by measuring impulse response using compact optical sensors", IEEE Transactions on Ultrasonics, Ferroelectrics and Frequency Control, 57(6), 2010, 1696-1700.
22. Zhang X, Qiang B and Greenleaf J. "Comparison of the surface wave method and the indentation method for measuring the elasticity of gelatin phantoms of different concentrations", Ultrasonics, 51, 2011, 157-164.
23. Madsen E L, Hobson M A, Shi H *et al*. "Tissue-mimicking agar/gelatin materials for use in heterogeneous elastography phantoms", Physics in Medicine and Biology, 50, 2005, 5597-5618.
24. Yang T H J. "Structure-property relationships in biological tissues", PhD Thesis, Heriot-Watt University, 2007.
25. Okamoto R J, Clayton E H and Bayly P V. "Viscoelastic properties of soft gels: comparison of magnetic resonance elastography and dynamic shear testing in the shear wave regime". Physics in Medicine and Biology, 56(19), 2011, 6379-6400
26. Liang X, Oldenburg A L, Crecea V *et al*. "Optical micro-scale mapping of dynamic biomechanical tissue properties", Optics Express, 16(15), 2008, 11052-11065.
27. Peters A, Chase J G and Van Houten E E W. "Digital image elasto-tomography: mechanical property estimation of silicone phantoms", Medical and Biological Engineering and Computing, 46, 2008, 205-212.
28. Santawisuk W, Kanchanavasita W, Sirisinha C *et al*. "Dynamic viscoelastic properties of experimental silicone soft lining materials", Dental Materials Journal, 29(4), 2010, 454-460.

29. Hao L, Shi Z and Zhao X. “Mechanical behaviour of starch/silicone oil/silicone rubber hybrid electric elastomer”, Reactive and Functional Polymers, 69, 2009, 165-169.

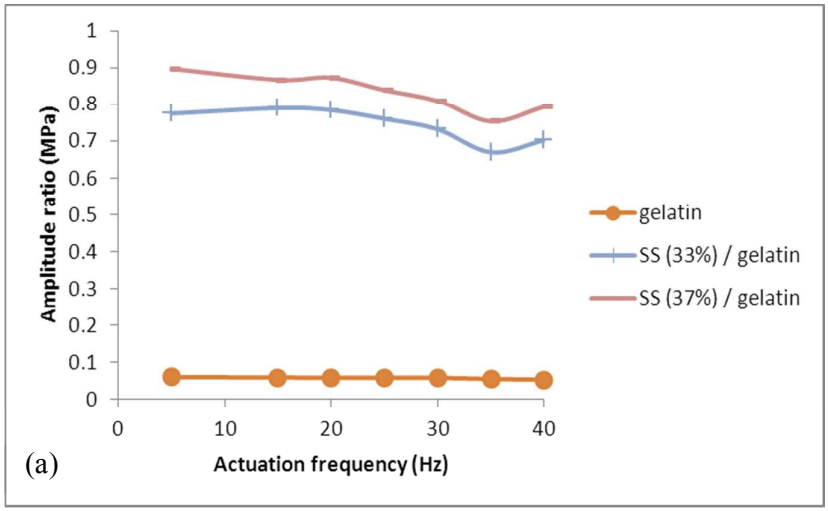

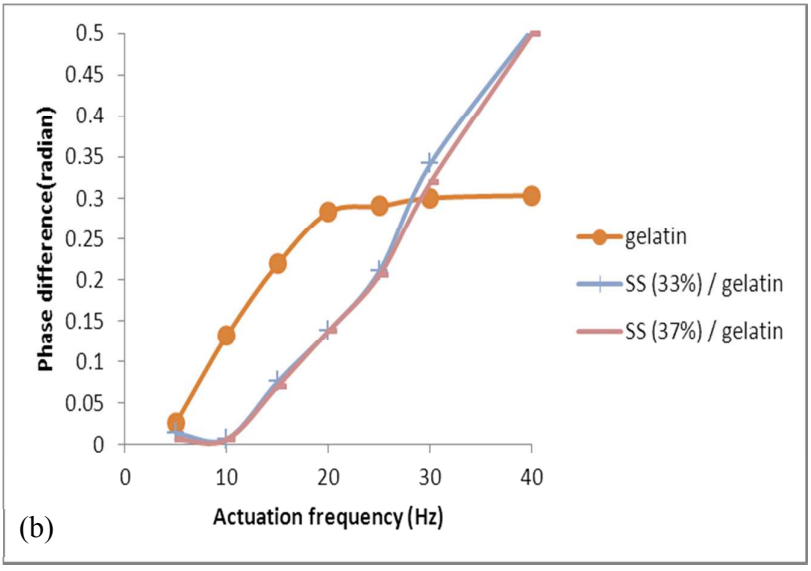

Figure 11: Effect of sponge reinforcement on the modulus of gelatin; (a) amplitude ratio, (b) phase difference.